The cusphere

M. Fernández-Guasti[a]

[a]Laboratorio de Óptica Cuántica, Depto. de Física, CBI, Universidad Autónoma Metropolitana - Iztapalapa, 09340 CDMX, A.P. 55-534, MEXICO

ARTICLE HISTORY
Compiled February 12, 2023

Abstract
A cusphere, portmanteau of cube and sphere, is the constant magnitude surface in imaginary scator algebra. The computer renderings exhibit a fascinating geometry with great aesthetic value. The scator space in 1+2 dimensions, is endowed with a scalar (real) and two hyper-imaginary components that can be represented in the three orthogonal axes of Euclidean space. A myriad of plane curves are obtained on the cusphere surface: Families of ellipses, circles and lemniscatae are three of the familiar ones. There are also less conventional ones, like four pointed stars and squircles. Implicit as well as parametric equations of these curves are derived. The three dimensional geometrical object is explored from different perspectives.

KEYWORDS
Scator algebra; isometric surfaces; hypercomplex magnitude;

1. Introduction

The relationships between geometric figures and our surrounding world has fascinated mankind from the outset of abstract thought. Geometrical forms such as the triangle, has a profound meaning to the Rarámuri culture in Northern Mexico (Sánchez and Galván, 2008). The circle and the square have been highly relevant geometrical shapes to different civilizations. On their own, they were praised by the Pythagorean school and later on by Plato and Aristotle. In conjunction, they are represented in many Tsukubai, washbasins in holy temples in Japan. An exceptional example for its harmony is the Tsukubai in the Ryōan-ji temple in Kyoto. The Vitruvian man of Leonardo again draws on these two figures to establish the proportions of the human body according to the Roman ideal of Vitruvius. A circle can be topologically transformed into a square and viceversa. The squircle equation[1] is one way to describe such a transformation (Fernández-Guasti, 1992)

$$x^2 + y^2 - \frac{s_\square^2}{r^2} x^2 y^2 = r^2, \tag{1}$$

CONTACT M. Fernández-Guasti. Email: mfg@xanum.uam.mx, url: https://luz.izt.uam.mx
[1] https://www.johndcook.com/blog/2022/10/27/variant-squircle/

subject to the restriction $x^2, y^2 \leq r^2$. When the squareness parameter $s_\square = 0$, the equation for a circle of radius r is obtained; Whereas a squarenes $s_\square = 1$, produces a square with sides equal to $2r$. The family of intermediate curves have been named squircles (Fernández-Guasti et al., 2005). They can be roughly described as a square with blunt corners (Weisstein, 2011). This shape has been used in design, particularly in squircle shaped touchpad buttons and icons in cell phones[2]. Squircles are more pleasing figures for these purposes rather than circles, that look demode, or squares that often give a too hard impression. Squircles have also been used to map circular onto square images (Fong, 2019; Bernabé et al., 2022). These curves have also been successfully extended to surfaces embedded in three dimensional space. For example, sphubes are intermediate figures between a sphere and a cube (Fong, 2018). Tiling of hyperbolic patterns is another fine example (Fong and Dunham, 2022).

This communication explores a three dimensional figure named a *cusphere*[3]. Rather than transforming a circle into a square with blunt corners and eventually with sharp ones, like in the previous description, these geometrical curves coexist simultaneously in the cusphere surface. However, these and other curves are not quite discernible at first sight. Nonetheless, their embedding within the surface may well play a role in the pleasing perception of the body.

In the next section, the elements and magnitude of *cuspheric* scator algebra are introduced. Constant magnitude surfaces embedded in three dimensions, that is, cuspheres in $\mathbb{S}^{1+2}$ scator space, are depicted. The orthographic projections of this figure are shown in subsection 2.1. A polar representation of scator numbers that lends itself for a direct parametric visualization, is presented in 2.2. Segments of the cusphere are shown in 2.3. Section 3 is devoted to curves generated by the intersection of a plane with the cusphere. In this way, ellipses (Subsec.3.1), lemniscatae and butterfly wings shaped curves (Subsec.3.2), four pointed stars (Subsec.3.3) and squircle-like curves (Subsec.3.4) are obtained. Conclusions and the quest for the construction of a physical object are undertaken in the last section.

2. The cusphere

The cusphere object emerged from the study and geometric representation of scator algebra. The geometry of a space is often defined in terms of the figure produced by a constant metric in such a space[4]. For example, hyperbolic geometry discovered by N. Lobatchevski, produce hyperbolic sheets that became renowned in the Minkowski description of special relativity. The graphic artist M. C. Escher produced some remarkable works depicting familiar objects within a hyperbolic geometry. Scator geometry is a nascent geometry with two branches: the hyperbolic scator version that has been successfully used to describe deformed Lorentz transformations (Fernández-Guasti, 2014) and the cuspheric scator version that has been used to describe celestial trajectories and choreographic motions and is a promising route to reduction theories in quantum mechanics. The cusphere, just like a sphere or a hyperboloid of revolution, is a fascinating object. These objects, so to speak, shine on their own and have an intrinsic aesthetic value. However, their relevance is greatly enhanced due to their relationship with the topology of a geometrical space and its concomitant algebraic structure. The relevance is further increased if these properties have a physical meaning or correspond to a physical scenario. The interplay between the cusphere geometry and its relationship with analytic

[2] https://en.wikipedia.org/wiki/Squircle

[3] The name 'cusfera' has been used in the spanish translation (Marmolejo, 2017)

[4] The notion of space here described may involve time. In physics the compound word space-time is often used, labeling time explicitly in addition to three dimensional space.

geometry and the scator structure is described in the appendix. The origin of the cusphere surface becomes apparent from this description.

Sca-tor numbers have elements with one *sca*-lar component and arbitrary direc-*tor* component terms, two in $1+2$ dimensions. From a conceptual point of view, the scalar component does not possess the quality of direction whereas the director components do. From a mathematical point of view, the scalar component behaves as an overall scaling factor. The director elements possess sense and direction, that is, they can be viewed as oriented line segments, somewhat similar to vector elements. However, vectors are not a subset of the scator set. A scator number $\overset{o}{\varphi} \in \mathbb{S}^{1+2}$ can be written as a sum of three terms

$$\overset{o}{\varphi} = s + x\check{\mathbf{e}}_x + y\check{\mathbf{e}}_y, \tag{2}$$

where $s \in \mathbb{R}$ is the scalar component and $x, y \in \mathbb{R}$ are the coefficients of the director components $\check{\mathbf{e}}_x, \check{\mathbf{e}}_y \notin \mathbb{R}$ respectively. The nature of the $\check{\mathbf{e}}_x, \check{\mathbf{e}}_y$ units is expounded in the appendix, they are hyper-imaginary units that satisfy $\check{\mathbf{e}}_x\check{\mathbf{e}}_x = -1$, $\check{\mathbf{e}}_y\check{\mathbf{e}}_y = -1$. An overhead oval is used in order to stress the scator nature of the number, *i.e.* $\overset{o}{\varphi}$. Scator algebra elements in $1+2$ dimensions can be portrayed in our familiar Euclidean three dimensional space in a similar fashion to complex numbers pictured in Argand diagrams. The scalar component is represented in one spatial axis (although it does not possess the quality of direction) and the two hyper-imaginary components are represented in the other two spatial axes of three dimensional space. The director coefficient, say $|x|$ or $|y|$, represents the magnitude of the component and the unit director, say $\check{\mathbf{e}}_x$ or $\check{\mathbf{e}}_y$, account for their direction. It should be kept in mind that the topology of scator objects in scator space differs from their Euclidean counterpart, although some of their features can be represented in this familiar space.

The *cusphere surface* is the constant scator magnitude surface. Its implicit equation, derived in the appendix is,

$$s^2 + x^2 + y^2 + \frac{x^2y^2}{s^2} = \text{constant}. \tag{3}$$

The constant plays the role of an overall scaling factor. This surface, depicted in figure 1, involves three variables s, x, y; the above equation establishes a relationship between them that leaves only two degrees of freedom. In $\mathbb{S}^{1+2}$, this two dimensional surface is embedded in a three dimensional space. The surface is smooth and both, pleasing and intriguing to the sight. There are some symmetries that strike the observer even at first glance. One of them is the mirror image of two halves of the volume that are joined at a cross with equal sides. There are also right-left and up-down symmetries; these are more clearly seen in figure 3, where segments of the whole figure are isolated. However, there are also some, not so evident or hidden symmetries. For example, the complete figure can be reproduced by the appropriate shift of an ellipse with $\sqrt{2}$ axes ratio, as we shall see in section 3.1. Trajectories along the surface can be performed so that the slope varies continuously. This property allows for smooth, well behaved curves. This is particularly interesting at the crossing points from one half to the other. At any of these points, the slope is continuous if the trajectory moves from one face to the opposite face at the crossing point. At the four extremes of the cross, the slope is continuous and equal for any of the faces. These features make the eye wander seamlessly through the different regions of the surface.

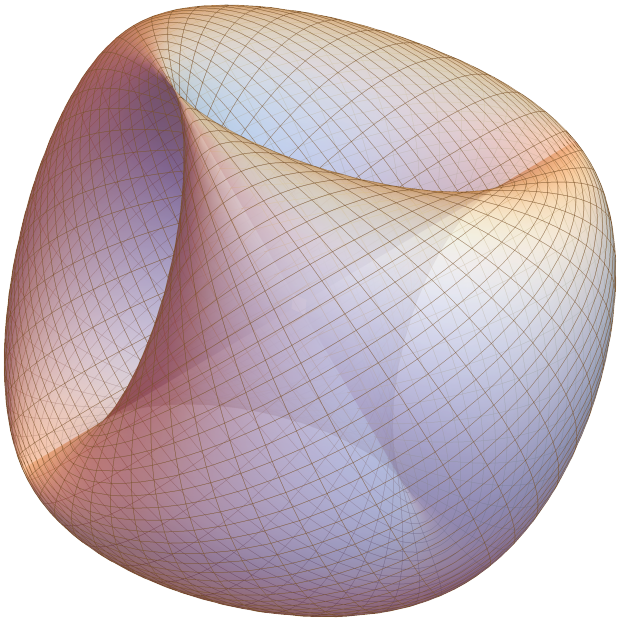

Figure 1. Cusphere, scator isometric surface in three dimensions for the $\mathbb{S}^{1+2}$ set.

2.1. Shadows

If the term $\frac{x^2y^2}{s^2}$ were not present in the scator magnitude (3), the result would be the familiar Euclidean metric. A way to eliminate this term is to consider $1+1$ dimensions. Then, either x or y is zero and the constant scator square magnitude (3) becomes $s^2+x^2=$ const. or $s^2+y^2=$ const. Thus, the cusphere surface exhibits circular projections in the $s,\check{\mathbf{e}}_x$ and $s,\check{\mathbf{e}}_y$ planes. However, the projection in the $\check{\mathbf{e}}_x,\check{\mathbf{e}}_y$ plane has been shown to be a square (Fernández-Guasti and Zaldívar, 2013). The orthographic projections of the cusphere are depicted in figure 2. The circle and the square are thus encoded within the cusphere surface, although it is not evident that they are there until the projections are observed. The circular projection shadows are also obtained at the planes within the cusphere when x or y are zero. However, the square projection does not lie on a plane in the cusphere surface. Thus, it cannot be obtained from the intersection of a plane with the cusphere. Four orthogonal planes tilted at 45° with respect to the $\check{\mathbf{e}}_x,\check{\mathbf{e}}_y$ axes, tangent to the cusphere are required to obtain the square on this surface. It requires certain experience with 3D forms to imagine the shadow of an smooth object that has filled circles in two orthogonal directions but a filled square in the remaining orthogonal direction.

2.2. Multiplicative or polar representation

There is a multiplicative representation of scators akin to the polar representation of complex numbers extended to three dimensions,

$$\overset{o}{\varphi}=\varphi_0 e^{\varphi_x\check{\mathbf{e}}_x}e^{\varphi_y\check{\mathbf{e}}_y}, \tag{4}$$

where e is the complex exponential function. φ_0 is the scator magnitude, φ_x is the angle between s and the $\check{\mathbf{e}}_x$ axis, φ_y is the angle between s and the $\check{\mathbf{e}}_y$ axis. The addition theorem

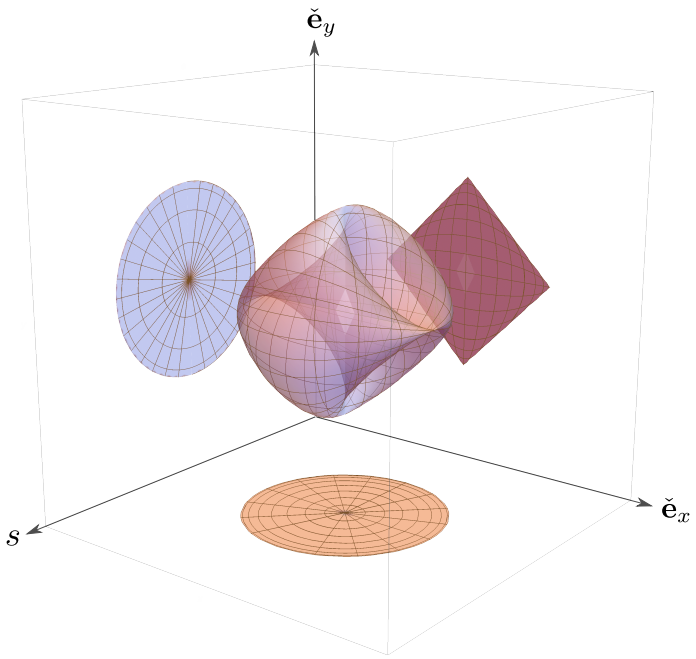

Figure 2. Cusphere orthographic projections. Filled circles are obtained in the $s, \check{\mathbf{e}}_x$ and $s, \check{\mathbf{e}}_y$ planes, whereas a filled square is obtained in the $\check{\mathbf{e}}_x, \check{\mathbf{e}}_y$ plane (rotated 45° with respect to the axes).

for exponents does not hold for scators with different director components, i.e. $e^{\varphi_x \check{\mathbf{e}}_x} e^{\varphi_y \check{\mathbf{e}}_y} \neq e^{\varphi_x \check{\mathbf{e}}_x + \varphi_y \check{\mathbf{e}}_y}$. However, it does hold for equal component coefficients $e^{\varphi_1 \check{\mathbf{e}}_x} e^{\varphi_2 \check{\mathbf{e}}_x} = e^{(\varphi_1+\varphi_2)\check{\mathbf{e}}_x}$ or $e^{\varphi_1 \check{\mathbf{e}}_y} e^{\varphi_2 \check{\mathbf{e}}_y} = e^{(\varphi_1+\varphi_2)\check{\mathbf{e}}_y}$. The multiplicative (4) and additive (2) representations of scators are related by

$$\overset{o}{\varphi} = \varphi_0 e^{\varphi_x \check{\mathbf{e}}_x} e^{\varphi_y \check{\mathbf{e}}_y} = \varphi_0 \cos\varphi_x \cos\varphi_y + \varphi_0 \cos\varphi_y \sin\varphi_x \check{\mathbf{e}}_x + \varphi_0 \cos\varphi_x \sin\varphi_y \check{\mathbf{e}}_y \\ = s + x\check{\mathbf{e}}_x + y\check{\mathbf{e}}_y. \quad (5)$$

The parametric representation of the cusphere requires $\varphi_0 =$ constant. A unit magnitude cusphere $\varphi_0 = 1$, is then parametrically described by

$$\overset{o}{\varphi}_{\text{unit cusphere}} = \cos\varphi_x \cos\varphi_y + \cos\varphi_y \sin\varphi_x \check{\mathbf{e}}_x + \cos\varphi_x \sin\varphi_y \check{\mathbf{e}}_y. \quad (6)$$

Computer generated cuspheres can be readily produced from this equation, i.e. in Mathematica: `ParametricPlot3D[{Cos[`φ_x`]Cos[`φ_y`],Cos[`φ_y`]Sin[`φ_x`],Cos[`φ_x`]Sin[`φ_y`]},{`φ_x`,0,2Pi},{`φ_y`,0,2Pi}]`.

2.3. Blend between the line and the arc: Segments of cusphere

To visualize the cusphere surface, consider one half of the complete figure 3a, restricted to a negative scalar component $s < 0$, shown in figure 3b. If we further restrict to the upper half plane in the $\check{\mathbf{e}}_y$ direction (figure 3c), and also the negative half plane in the $\check{\mathbf{e}}_x$ direction, the curved surface shown in figure 3d is obtained. Eight such identical pieces put together, make the whole cusphere. The rim of this segment, that accounts for an eighth of a cusphere, has two straight lines (in the x and y axes) and two arcs of a circle (in the $s, \check{\mathbf{e}}_x$ and $s, \check{\mathbf{e}}_y$ planes). This

surface thus produces a blend between two segments of straight lines and two arcs of a circle. A careful composition between lines and curves is required to achieve an aesthetic result. To put it differently, straight lines go well together and so do curved shapes. However, it is quite challenging to put straight lines and curves together in an artistic way. From a physical point

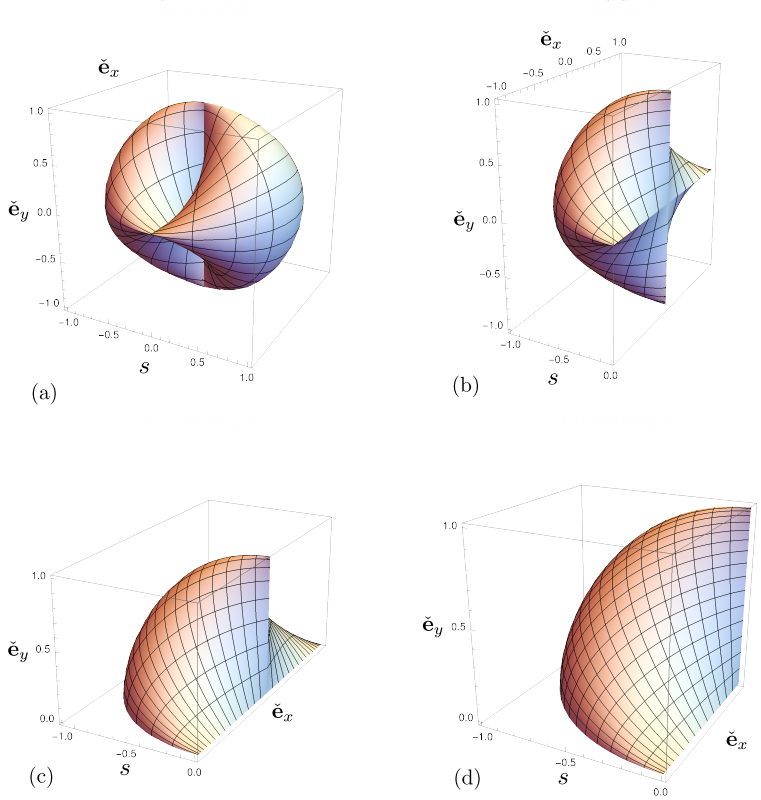

Figure 3. Segments of the cusphere seen from a different perspective: (a) Complete figure, (b) Half section with $s \leq 0$, (c) Quarter section $s \leq 0$, $y \geq 0$, (d) Eighth section $s \leq 0$, $x \leq 0$, $y \geq 0$.

of view, the most elementary trajectories are the straight line and the circular path. The former is described by a body in the absence of forces whereas the latter, when uniform, is the only accelerated system where the magnitude of the velocity is constant. This is achieved by having the acceleration orthogonal to the velocity at all times. From a geometrical point of view, the straight line is the shortest distance between two points in Euclidean geometry. The circle in two dimensions or a sphere in three dimensions are the geometrical objects with constant Euclidean metric with respect to a point, that is, the set of points equidistant to a reference point. Thus, the blend between the line and the arc in a smooth surface relies on the fusion of two of the most fundamental one dimensional geometrical objects.

3. Plane curves on the cusphere surface

Inasmuch as geodesics and other types of curves are relevant to understanding many properties of the sphere or other curved surfaces, curves in the cusphere are of paramount importance to elucidate the nature of this surface. The concept of vicinity, that is, of a set of points being near of far from another point, rely on the understanding of the cusphere properties. Closed or open cuspheres are the counterpart of closed or open balls in metric spaces. The study

of elliptical and lemniscatae curves were motivated by the scator description of celestial trajectories and novel choreographic motions Fernández-Guasti (2023). Squircle like curves have important applications in hardware (buttons in electronic devices) as well as in frontend image (virtual icons and buttons) industrial and graphics design. There are different families of curves that arise from the intersection of a plane with the cusphere surface. The procedure is reminiscent of the conics that arise from the intersection of a plane with a double cone. The first subsection considers planes that generate circles and ellipses. Thereafter, in the following three subsections, lemniscatae, four point stars and squircles are described. The description is not exhaustive of the types of plane curves that are achievable but tries to give a coup d'oeil at various possibilities.

3.1. Ellipses

Let a, b be constants and let the φ_x angle be fixed by the equations $a = \varphi_0 \sin\varphi_x$ and $b = \varphi_0 \cos\varphi_x$. The scator $\overset{o}{\varphi}_{\text{elli}}$, from (5), is then

$$\overset{o}{\varphi}_{\text{elli}} = \underbrace{b\cos\varphi_y}_{s} + \underbrace{a\cos\varphi_y}_{x}\check{\mathbf{e}}_x + \underbrace{b\sin\varphi_y}_{y}\check{\mathbf{e}}_y. \tag{7}$$

This expression is a parametric representation of an ellipse in the $\varphi_x =$ constant plane (Fernández-Guasti, 2023). It is also an ellipse in the $\check{\mathbf{e}}_x, \check{\mathbf{e}}_y$ plane, $(a\cos\varphi_y, b\sin\varphi_y)$. Circles of radius b are produced in the $s, \check{\mathbf{e}}_y$ projection, $(b\cos\varphi_y, b\sin\varphi_y)$ and line segments with slope $\frac{a}{b}$ are produced in the $s, \check{\mathbf{e}}_x$ projection $(b\cos\varphi_y, a\cos\varphi_y)$. The plane with $\varphi_x = \arctan\frac{a}{b}$, is shown in semitransparent brown in figure 4a. Through a rotation of $\theta = \varphi_x - \frac{\pi}{2}$ in the $s, \check{\mathbf{e}}_x$ plane,

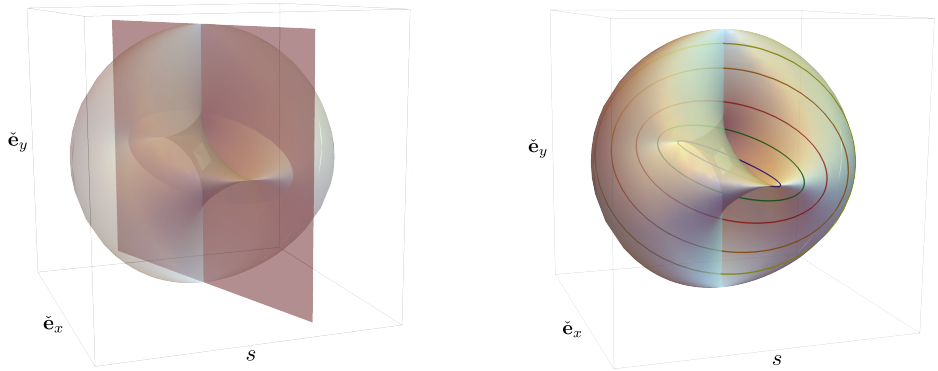

(a) Ellipses arise from the intersection with planes containing the $\check{\mathbf{e}}_y$ axis, and different angles in the $s, \check{\mathbf{e}}_x$ plane.

(b) Ellipses with different eccentricities at various angles in the $s, \check{\mathbf{e}}_x$ plane (intersecting planes not shown).

Figure 4. Families of ellipses with varying semi-minor axis on the cusphere surface. The intersecting planes rotate about the $\check{\mathbf{e}}_y$ axis.

$\overset{o\,\prime}{\varphi}_{\text{elli}} = (b\cos\theta + a\sin\theta)\cos\varphi_y + (a\cos\theta - b\sin\theta)\cos\varphi_y\check{\mathbf{e}}_x + b\sin\varphi_y\check{\mathbf{e}}_y$, the equation for the ellipse in the inclined plane is obtained

$$\overset{o\,\prime}{\varphi}_{\text{elli}} = \varphi_0\cos\varphi_y\check{\mathbf{e}}'_x + b\sin\varphi_y\check{\mathbf{e}}_y,$$

where $a' = \varphi_0$, $b' = b = \varphi_0 \cos\varphi_x$ and $\check{\mathbf{e}}'_x$ is the direction of the inclined plane. The ellipse eccentricity is $e = \sqrt{1 - \frac{b'^2}{a'^2}}\sqrt{1-\cos^2\varphi_x} = \sin\varphi_x$. Several coloured ellipses with different φ_y angles are shown in figure 4b. If $\varphi_x = 0$, $a' = b$, the eccentricity is zero and a circle is thus obtained. If $\varphi_x = \frac{\pi}{2}$, $b = 0$, the eccentricity is one and a line segment is obtained. Analogous figures are obtained as a function of φ_x for planes that rotate about the $\check{\mathbf{e}}_x$ axis if the φ_y angle is fixed at different constant values.

3.1.1. Four tangent ellipses

A unit magnitude cusphere is assumed hereafter, $\left\|\overset{o}{\boldsymbol{\varphi}}\right\| = \varphi_0 = 1$. The equation of a straight line at 45° is given by $y = \pm x + c$. Such a line should cross the $\check{\mathbf{e}}_y$ axis at $c = \pm 1$ in order to be tangent to the cusphere. These lines, evaluated for all s, gives rise to 45° planes. Substitution of $y = \pm x \pm 1$ in terms of the scator angles gives $\cos\varphi_x \sin\varphi_y = \pm\cos\varphi_y \sin\varphi_x \pm 1$, that can be rewritten as $\sin(\varphi_y \mp \varphi_x) = \pm 1$. The angle φ_y is then $\varphi_y = \pm\varphi_x \pm \frac{\pi}{2}$. The parametric equations of the four tangent ellipses to the cusphere are obtained from substitution of $\varphi_y = \pm\varphi_x \pm \frac{\pi}{2}$ in the unit cusphere expression (6),

$$\overset{o}{\boldsymbol{\varphi}}_{\text{4-ellipses}} = \pm\cos\varphi_x \sin\varphi_x \pm \sin^2\varphi_x\, \check{\mathbf{e}}_x + \cos^2\varphi_x\, \check{\mathbf{e}}_y. \tag{8}$$

The four sign combinations render the ellipses depicted in figure 5a. The semi-axes ratio of the ellipses is fixed and equal to $\frac{\text{major axis}}{\text{minor axis}} = \sqrt{2}$.

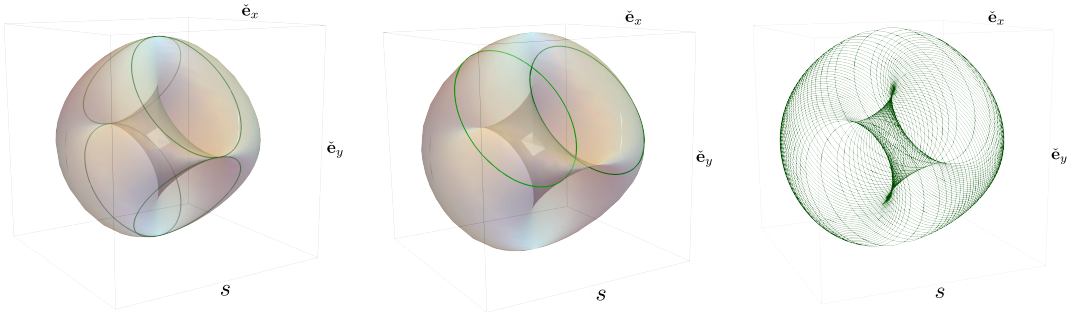

(a) Four ellipses are obtained in the $\pm\frac{\pi}{4}$ tangent planes given by Eq. (8).

(b) Two typical ellipses at $\frac{\pi}{4}$ in the $\check{\mathbf{e}}_x, \check{\mathbf{e}}_y$ plane intersecting the y axis at $y_0 = 0.7$.

(c) Ellipses at $\frac{\pi}{4}$ plane in the $\check{\mathbf{e}}_x, \check{\mathbf{e}}_y$ plane for many values of y_0.

Figure 5. Families of ellipses with fixed axes ratio on the cusphere surface.

3.1.2. *Double and multiple ellipses*

If the constant c takes an arbitrary value y_0 in the interval $(-1,1)$, recalling that $\cos(\arcsin y_0) = \pm\sqrt{1-y_0^2}$,

$$\overset{o}{\varphi}_{\pi/4} = \pm\left(\sqrt{1-y_0^2}\cos^2\varphi_x - y_0\sin\varphi_x\cos\varphi_x\right) + \left(\sqrt{1-y_0^2}\sin\varphi_x\cos\varphi_x - y_0\sin^2\varphi_x\right)\check{\mathbf{e}}_x + \left(\sqrt{1-y_0^2}\sin\varphi_x\cos\varphi_x + y_0\cos^2\varphi_x\right)\check{\mathbf{e}}_y. \quad (9)$$

The parametric plot of this expression describes two ellipses that degenerate into one at the tangent planes. As the value y_0 is spanned from 1 to 0, two ellipses, initially overlapped, separate laterally as shown in figure 5b for $y_0 = 0.7$. At $y_0 = 0$, the ellipses only meet at a tangent point situated at the origin. From 0 to -1, the ellipses come back closer intersecting at two points and eventually overlapping at the opposite tangent plane (shown in 5a). The shape of the ellipses remains invariant with semi-axes ratio of $\sqrt{2}$ for all y_0. Therefore, the cusphere surface can also be recreated in this way, with ellipses at 45° spanning from $-1 \leq y_0 \leq 1$, as depicted in figure 5c.

3.2. *Lemniscatae and papalotl*

The intersections of s,x planes with constant y (or s,y planes with constant x) and the cusphere produce figure of eight like curves as shown in figure 6a. Lemniscatae are obtained for large constant $y = y_c$ (or $x = x_c$) values different from zero. For $y_c = 0$, the curve becomes a circle as we have seen before. This result is reminiscent of the Bernoulli lemniscata as a particular case of the Cassini ovals. The scator polynomial is quartic in s but quadratic in x,

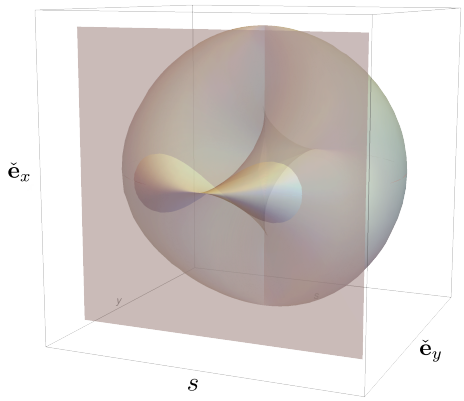

(a) Intersection of cusphere and the $y_c = 0.8$ constant plane.

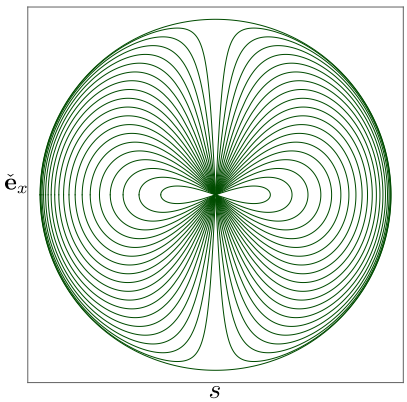

(b) Contour plot of cusphere at different constant $y = y_c$ planes.

Figure 6. Lemniscata curves are obtained for sections in the s,x plane for y_c large. However, when y_c is small, the curves resemble *papalotl* (butterfly wings in náhuatl) contours.

$$\left(s^2+x^2\right)\left(s^2+y_c^2\right)=s^2. \tag{10a}$$

In contrast, the Cassini ovals are quartic polynomials in both variables. In figure 6b, we show some of these curves for different values of y_c. If y_c is much smaller than the scator magnitude, the curves look more like butterfly wings, named papálotl in Aztec language. We should mention that only real points are being plotted. However, hidden symmetries are often obtained if the complex points of the lemniscate are also considered (Langer and Singer, 2010). To obtain the parametric representation, impose the condition $y_c=\cos\varphi_x\sin\varphi_y$ in the unit magnitude scator equation (6). The φ_y angle can thus be written in terms of φ_x, upon rearrangement

$$\overset{o}{\varphi}_{\text{lem-papalotl}}=\cos\varphi_x\sqrt{1-\frac{y_c^2}{\cos\varphi_x^2}}+\sin\varphi_x\sqrt{1-\frac{y_c^2}{\cos\varphi_x^2}}\,\check{\mathbf{e}}_x+y_c\,\check{\mathbf{e}}_y. \tag{10b}$$

Plots in the $s,\check{\mathbf{e}}_x$ plane for different values of the constant y_c, can be readily obtained from this expression. Analogous results are obtained in the $s,\check{\mathbf{e}}_y$ plane for different values of x_c.

3.3. Ek curves

Intersections of x,y planes and the cusphere produce rather different figures depending on the value of the constant $s=s_c$. A semitransparent blue plane with $s_c=0.3$ intersecting the cusphere is shown in figure 7a. If s_c is much smaller than the scator magnitude, four pointed star figures, named ek (star) or ek chaneb (four star) curves, are obtained as shown in figure 7b. An equilateral cross is obtained in the limit when $s_c\to 0$. The implicit curve

$$x^2+y^2+\frac{1}{s_c^2}x^2y^2+s_c^2=1, \tag{11a}$$

gives the ek curve for $0\leq s_c\leq 0.3$. The scator parametric curve, making the scalar component constant $s_c=\cos\varphi_x\cos\varphi_y$, from (6) is then

$$\overset{o}{\varphi}_{\text{ek/squircle}}=s_c+s_c\tan\varphi_x\,\check{\mathbf{e}}_x+\cos\varphi_x\sqrt{1-\frac{s_c^2}{\cos^2\varphi_x}}\,\check{\mathbf{e}}_y. \tag{11b}$$

A rotation of (11a) by $\frac{\pi}{4}$, gives

$$x'^2+y'^2+\frac{1}{4s_c^2}\left(y'^2-x'^2\right)^2=1-s_c^2. \tag{11c}$$

In the small s_c limit, truncated hyperbolae $y'^2-x'^2\approx 2s_c$ or $x'^2-y'^2\approx 2s_c$ are obtained. The curves are truncated because $x'^2+y'^2<1$. These hyperbolae make up for the main features of the ek sides shown in 7b. Four pointed star like images arise in different optical systems. Notably, the diffraction spikes in reflection telescopes due to the support of the secondary mirror.

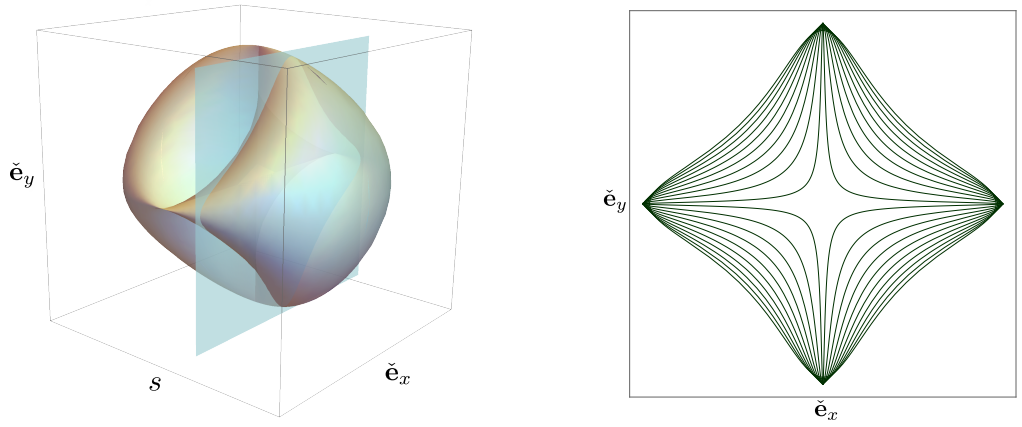

(a) Intersection of cusphere and the $s_c = 0.3$ constant plane.

(b) Contour plot of cusphere at different constant $0.01 \leq s \leq 0.3$ planes.

Figure 7. Ek (star in Mayan) curves are obtained for sections in the x, y plane for small s_c.

3.4. Squircle like curves

If the constant s_c is greater than x, y, the curves look like a square with blunt corners reminiscent of the squircle shape, as shown in figure 8. However, two relevant differences are, that the shape is rotated by $\frac{\pi}{4}$ compared with the squircle and the scale is reduced as the shape approaches the circle. The previous rotated equation (11c), has a negative term $-\frac{1}{2s_c^2}x'^2y'^2$, analogous to that obtained in the squircle equation (1). Thus the similarity of the curves for intermediate values of s_c. If $s_c \gg x, y$, the implicit curve (11a) becomes $x'^2 + y'^2 = 1 - s_c^2$, since the term $\frac{1}{4s_c^2}\left(y'^2 - x'^2\right)^2$ can be neglected. That is, a circle with radius $\sqrt{1 - s_c^2}$ is obtained. Notice that the radius is reduced as s_c increases. Therefore, the Euclidean metric is recovered if $s_c \gg x, y$. In $\mathbb{S}^{1+3}$, where three director components are included representing three dimensional space, a sphere is obtained in the $s_c \gg x, y, z$ limit. This result is particularly important because the Euclidean metric is enclosed in the scator magnitude. It is obtained in the limit when the scalar component is large compared with the director components. Hyperbolic scators are a sister algebra of cuspheric scators. They are particularly well suited to describe relativistic phenomena (Fernández-Guasti, 2020). Hyperbolic scators exhibit a similar limit to the one just described. They reproduce the relativistic Lorentz metric in the $1+1$ dimensions limit (Kobus and Cieśliński, 2017) and the Galilean classical mechanics limit for $s \gg x, y, z$.

4. Perspectives

The feasibility of a cuspheric physical object was of great concern ever since the first visualizations of the cusphere equation. To this end, the contours obtained in different directions (Figures 6b, 7b and 8b) were cut in foamy and superimposed to produce a crude version of different parts of the physical object. After careful study of the computer rendered screen visualizations of the cusphere from different points of view, a hand made terracotta model was constructed in two half pieces of 8 cm diameter each. This model is shown in figure 9. The invaluable guide of sculptor and physicist Dr. Alonso Fernández González, was essential

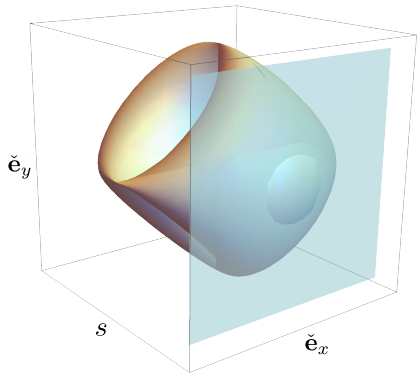

(a) Intersection of cusphere and the $s = 0.955$ constant plane.

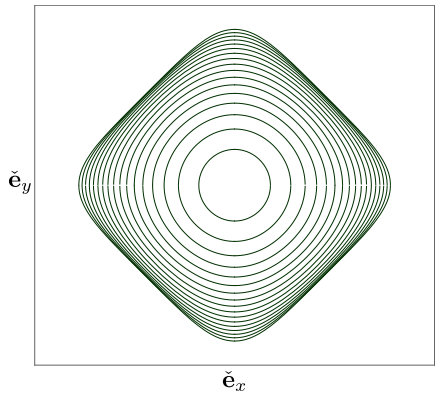

(b) Contour plot of cusphere at different constant $0.5 \leq s \leq 0.99$ planes.

Figure 8. Squircle-like curves are obtained for sections in the x,y plane for s_c large. The limit for $s_c \gg x,y$ is a circle, an important feature because in this limit the Euclidean norm is recovered.

Figure 9. Hand made terracotta version of the cusphere, $8 \times 8 \times 8$ cm. The distinctive trait of Dr. Alonso Fernández is imprinted in the sculpture.

to mould and bake the clay. A bronze cast of this figure was performed by foundry worker Rodrigo García in Cuernavaca, Morelos. The chipped half with blemishes was the one used to make the cast.

A 20 cm diameter cusphere version was produced in a 3D printer from the cusphere equation (3). A half segment of the cusphere was computer rendered in a stereolithography (Standard tessellation language) .stl file[5]. This file was used to produce two polymer halves in a 3D printer. The two pieces were glued together and coated with automotive paint. A photograph of the cusphere sculpture is shown in figure 10. The cusphere 3D object has also been referred to as a *scator metric sculpture*. It exhibits all the properties and characteristics mentioned in the previous sections, including the circular projections in two orthogonal directions while a square is produced in the remaining direction. To observe these projections, the observer needs to be appropriately located. Perspective and point of view are of paramount importance

[5]This file is included as supplementary material. It can also be provided on request.

Figure 10. Cusphere - 3D print (20 × 20 cm size)

to the experience of the individual. To put it boldly, you can see a square or a circle depending on where you stand. There are, of course, countless other silhouettes that are observed form intermediate positions between the orthogonal axes. It is worth mentioning that this state of affairs can also be translated into everyday life. What we see and the way we perceive the events and phenomena around us, strongly depend on where we are and the way we look at them.

There are interesting proposals concerning the cusphere that have not yet come to life. A cusphere time capsule of monumental dimensions ($2\text{m} \times 2\text{m} \times 2\text{m}$) has been proposed (Fernández-Guasti, 2013). The cusphere involves one scalar axis that has been naturally associated with a time variable. It is then all too natural to involve time in the cusphere experience. An interesting proposal of a large wire gridded public sculpture has now been proposed twice, by Dr. Gerardo Muñoz and an anonymous reviewer. Some inner features would then be available to spectators and children to explore. On the other hand, there are curves concealed in the cusphere three dimensional space with very interesting properties. One such curve, named the unitrix curve, is shown in figure 11. Its projections in the orthogonal planes produce the trifolium rose, Pascal's limaçon and Gerono's lemniscata. It is up to the reader to enrich these proposals and decide on the merits of the imaginary scators isometric surface, namely, the cusphere.

Acknowledgements

The author is greatly indebted to Labná Fernández-Eraña for her excellent suggestions and revision of several parts of the manuscript; and Alejandra Leonides-Zamora for penetrating comments from a designer's point of view. The editor and reviewers comments were also helpful to improve the quality of this work.

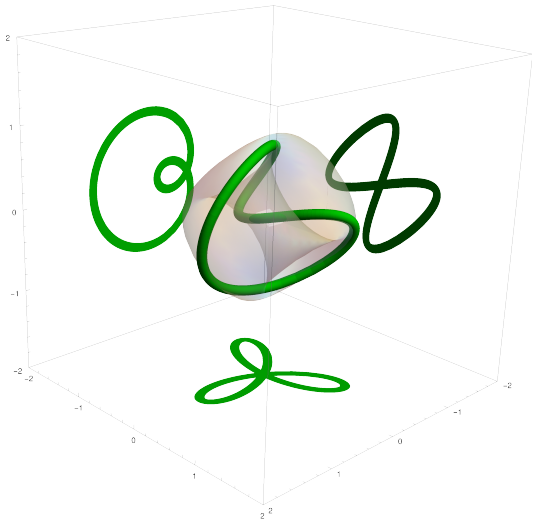

Figure 11. The unitrix curve is shown on the cusphere surface and its planar projections: The trifolium rose (bottom), Pascal's snail (left) and Gerono's lemniscata (right).

Nomenclature/Notation

Scator quantities are represented with an overhead oval, $\overset{o}{\varphi}$.

Unit directors are represented with a check and the appropriate subindex $\check{\mathbf{e}}_x$, $\check{\mathbf{e}}_y$. The check instead of a hat ($\hat{\mathbf{e}}_j\hat{\mathbf{e}}_j = 1$), stresses the negative square relationships, $\check{\mathbf{e}}_x\check{\mathbf{e}}_x = -1$ and $\check{\mathbf{e}}_y\check{\mathbf{e}}_y = -1$.

Appendix A. Cuspheric Scator Product and magnitude in $\mathbb{S}^{1+2}$

Scator algebra is an extension of complex algebra to higher dimensions, in particular a three dimensional space, labeled $1+2$ because it is endowed with one scalar component and two director components. The guiding principle for many novel algebraic systems, is to provide a structure that facilitates the description of diverse physical scenarios. Generalizations of algebraic structures beyond the real and complex numbers can no longer retain the sum and product commutative group properties. For example, the quaternion product is not commutative and octonions are neither commutative nor associative. The scator product is commutative but not associative. However, the hallmark of this algebra is that the scator product is not distributive over addition. In linear algebra, vectors cannot be added to scalars. In contrast, geometric algebras, 'mix' components with different grade, for example, scalars can be added to the vector components. This is also true for scators, where a scalar and director components can be added or multiplied. However, in scator algebra the scalar term becomes strictly necessary, a scalar component must be added to the director components in dimensions greater than 2.

The *scator set* $\mathbb{S}^{1+2}$, is the subset of $\mathbb{R}^{1+2}$ where the scalar component is non-zero if the two director components are non-zero (Fernández-Guasti, 2015),

$$\mathbb{S}^{1+2} = \left\{ \overset{o}{\varphi} \in \mathbb{R}^{1+2} : s \neq 0, \text{ if } xy \neq 0 \right\}, \tag{A1}$$

The scator sum is defined component-wise in $\mathbb{R}^{1+2}$. However, the scator product is only defined in the $\mathbb{S}^{1+2}$ subset.

Definition 1. The product of two scators, $\overset{o}{\alpha} = a_0 + a_x\check{\mathbf{e}}_x + a_y\check{\mathbf{e}}_y$ and $\overset{o}{\beta} = b_0 + b_x\check{\mathbf{e}}_x + b_y\check{\mathbf{e}}_y$ in $\mathbb{S}^{1+2}$ is,

if $a_0 b_0 \neq 0$,

$$\overset{o}{\alpha}\overset{o}{\beta} = a_0 b_0\left(1-\frac{a_x b_x}{a_0 b_0}\right)\left(1-\frac{a_y b_y}{a_0 b_0}\right) + a_0 b_0\left(1-\frac{a_y b_y}{a_0 b_0}\right)\left(\frac{a_x}{a_0}+\frac{b_x}{b_0}\right)\check{\mathbf{e}}_x + a_0 b_0\left(1-\frac{a_x b_x}{a_0 b_0}\right)\left(\frac{a_y}{a_0}+\frac{b_y}{b_0}\right)\check{\mathbf{e}}_y; \quad \text{(A2)}$$

if $a_0 = 0$, the scator $\overset{o}{\alpha} \in \mathbb{S}^{1+2}$ can only have a single non-vanishing director component, say $\overset{o}{\alpha} = a_l\check{\mathbf{e}}_l$. Its product times a scator $\overset{o}{\beta}$ with $b_0 \neq 0$, is

$$(a_x\check{\mathbf{e}}_x)\overset{o}{\beta} = -a_x b_x + b_0 a_x\check{\mathbf{e}}_x - \frac{a_x b_x b_y}{b_0}\check{\mathbf{e}}_y \quad \text{or} \quad (a_y\check{\mathbf{e}}_y)\overset{o}{\beta} = -a_y b_y + b_0 a_y\check{\mathbf{e}}_y - \frac{a_y b_y b_x}{b_0}\check{\mathbf{e}}_x; \quad \text{(A3)}$$

if $a_0 = b_0 = 0$, at most one of the director components of the scators $\overset{o}{\alpha}$ and $\overset{o}{\beta}$ is nonzero, say a_l and b_j respectively, the product $\overset{o}{\alpha}\overset{o}{\beta}$ is then

$$(a_x\check{\mathbf{e}}_x)(b_x\check{\mathbf{e}}_x) = -a_x b_x, \quad (a_y\check{\mathbf{e}}_y)(b_y\check{\mathbf{e}}_y) = -a_y b_y, \quad (a_x\check{\mathbf{e}}_x)(b_y\check{\mathbf{e}}_y) = (a_y\check{\mathbf{e}}_y)(b_x\check{\mathbf{e}}_x) = 0 \quad \text{(A4)}$$

This product definition is consistent with the multiplicative to additive representation (5) and sum of exponents for equal component coefficients. According to (A4), the units $\check{\mathbf{e}}_x$ or $\check{\mathbf{e}}_y$ are then just like an imaginary unit, i.e. $\check{\mathbf{e}}_x\check{\mathbf{e}}_x = -1$, $\check{\mathbf{e}}_y\check{\mathbf{e}}_y = -1$ with orthogonality between them $\check{\mathbf{e}}_x\check{\mathbf{e}}_y = 0$. However, if the elements of the factors involve several components, definitions (A2)-(A3) have to be invoked. The scator product is commutative and, excluding zero, all elements have inverse. However, it is not associative if the product of any two factors has zero scalar component. *Conjugation* is the main second order involution of a scator $\overset{o}{\varphi}$. It is given by the negative of the director components while the scalar component remains unaltered $\overset{o}{\varphi}^* \equiv s - x\check{\mathbf{e}}_x - y\check{\mathbf{e}}_y$. The product of a scator times its conjugate establishes its square magnitude. For a scator with non zero scalar component $s \neq 0$,

$$\left\|\overset{o}{\varphi}\right\|^2 = \overset{o}{\varphi}\overset{o}{\varphi}^* = s^2\left(1+\frac{x^2}{s^2}\right)\left(1+\frac{y^2}{s^2}\right) + 0\check{\mathbf{e}}_x + 0\check{\mathbf{e}}_y. = s^2 + x^2 + y^2 + \frac{x^2 y^2}{s^2}, \quad \text{(A5)}$$

and if the scalar component of the scator is zero, there is only one director component in $\mathbb{S}^{1+2}$, either $\left\|\overset{o}{\varphi}\right\|^2 = x^2$ or $\left\|\overset{o}{\varphi}\right\|^2 = y^2$. This is the genesis of the cusphere equation in $\mathbb{S}^{1+2}$.

Notice that the usual definition of complex numbers is obtained if the factors have a director component only in $\check{\mathbf{e}}_x$ or $\check{\mathbf{e}}_y$. From (A2), it is clear that the scator product is not distributive, i.e.

$$(a_0 + a_x\check{\mathbf{e}}_x + a_y\check{\mathbf{e}}_y)(b_0 + b_x\check{\mathbf{e}}_x + b_y\check{\mathbf{e}}_y) \neq a_0 b_0 + a_x b_0\check{\mathbf{e}}_x + a_y b_0\check{\mathbf{e}}_y + a_0 b_x\check{\mathbf{e}}_x - a_x b_x + a_0 b_y\check{\mathbf{e}}_y + a_x\check{\mathbf{e}}_x - a_y b_y.$$

Nonetheless, a graded algebra introducing bivector type units can be implemented to recover distributivity analogous to hyperbolic scator algebra (Cieśliński and Kobus, 2020).

Scator addition is defined in $\mathbb{R}^{1+2}$, whereas multiplication is defined in $\mathbb{S}^{1+2}$ a subset of $\mathbb{R}^{1+2}$ where the scalar component is not zero if the director components do not vanish. To appraise the implications of defining the two operations in two different sets, recall what happens in the real set and the multiplicative inverse. If we evaluate the inverse of $a-a$, $a \in \mathbb{R}$, it is not in the reals $\frac{1}{a-a} \notin \mathbb{R}$. Dividing by zero is a 'forbidden' operation in the real set because infinity is not in the reals. (If we use the extended real set, including infinity, then addition group properties are violated). For this reason, zero is excluded from the product group properties in the reals. Mutatis mutandis, in scator algebra, in order to have scator products that do not give infinite results, not only one element (zero in the reals) but the set of scators with null scalar if $xy \neq 0$, also has to be excluded.

References

Bernabé, S., García, G., Carrasco, V. M. S., and Vaquero, J. M. (2022). SunMap: A solar image processing software for obtaining synoptic maps. *Solar Physics*, 297(8).

Cieśliński, J. L. and Kobus, A. (2020). On the product rule for the hyperbolic scator algebra. *Axioms*, 9:55.

Fernández-Guasti, M. (1992). Analytic geometry of some rectilinear figures. *Int. Jour. of Math. Ed. in Sci. & Tech.*, 23(6):895–901.

Fernández-Guasti, M. (2013). Escultura métrica: escatores imaginarios en 1+2 dimensiones y la escala humana. In Dieterich, H., editor, *Cyberspace and the Quest for a Materialistic Epistemology of Liberation*, page 141–148. Druck and Verlag GmbH.

Fernández-Guasti, M. (2014). Time and space transformations in a scator deformed Lorentz metric. *European Physical Journal - Plus*, 129(195):1–10.

Fernández-Guasti, M. (2015). A non-distributive extension of complex numbers to higher dimensions. *Adv. Appl. Clifford Algebras*, 25:829–849.

Fernández-Guasti, M. (2020). Composition of velocities in a scator deformed Lorentz metric. *Eur. Phys. J. Plus*, 135:542.

Fernández-Guasti, M. (2023). *Advances in number theory and applied analysis*, chapter 9: The components exponential function in scator hypercomplex space: planetary elliptical motion and three body choreographies. World Scientific, Singapore.

Fernández-Guasti, M., Cobarrubias, A. M., Carrillo, F. J. R., and Cornejo-Rodríguez, A. (2005). LCD pixel shape and far field diffraction patterns. *Optik*, 116:265–269.

Fernández-Guasti, M. and Zaldívar, F. (2013). An elliptic non distributive algebra. *Adv. Appl. Clifford Algebras*, 23(4):825–835.

Fong, C. (2018). Squircular calculations. arXiv:1604.02174v3.

Fong, C. (2019). Analytical methods for squaring the disc. arXiv:1509.06344v4.

Fong, C. and Dunham, D. (2022). A Sham Schwarz surface based on a squircle. In Reimann, D., Norton, D., and Torrence, E., editors, *Proceedings of Bridges 2022: Mathematics, Art, Music, Architecture, Culture*, pages 25–32, Phoenix, Arizona. Tessellations Publishing.

Kobus, A. and Cieśliński, J. L. (2017). On the geometry of the hyperbolic scator space in 1+2 dimensions. *Advances in Applied Clifford Algebras*, 27(2):1369–1386.

Langer, J. C. and Singer, D. A. (2010). Reflections on the lemniscate of Bernoulli: the forty-eight faces of a mathematical gem. *Milan Journal of Mathematics*, 78(2):643–682.

Marmolejo, E. (2017). Conexiones entre conceptos matemáticos y otras áreas del conocimiento: Sumem (rdu). *Revista Digital Universitaria*, 18(6).

Sánchez, A. G. and Galván, F. M. (2008). *Geometrías de la imaginación: Diseño e iconografía Chihuahua*. Instituto Chihuahuense de la Cultura.

Weisstein, E. W. (2011). Squircle.